

Galloping of overhead transmission lines in gusty wind

Takeshi Ohkuma[†]

*Department of Architecture, Kanagawa University, 3-27-1 Rokkaku-bashi, Kanagawa-ku,
Yokohama 221-0802, Japan*

Hisao Marukawa[‡]

*Urban Environment Research Center, Izumi Sohken Engineering Co., Ltd.
51 Minami-sode, Sodegaura, Chiba 299-0268, Japan*

Abstract. To develop galloping suppression devices, it is important to understand the effects of wind turbulence on galloping and to establish an evaluation method which takes 'large conductor deformations' into account. This paper introduces some findings on galloping in gusty wind obtained by numerical simulation using a model based on the Mogami Test Line of the Tokyo Electric Power Co. The equations of motion of the conductor are based on the Lagrangian formulations by Simpson, and they are made discrete in accordance with a finite element method.

Key words: galloping; overhead transmission lines; wind turbulence; numerical simulation.

1. Introduction

Galloping of overhead transmission lines has been under investigation for a long time in the industrial aerodynamics field (IEEEJ 1979, EPRI 1980), and is still awaiting solution. In particular, galloping suppressing devices with higher applicability and reliability are in strong demand to enable structural changes of overhead transmission line systems resulting from increased carrying capacity and longer spans. This will become feasible with the development of analytical techniques using high performance computers, and development of wind engineering as well as industrial aerodynamics.

To achieve a solution, it is important to understand the effects of wind turbulence on galloping and to establish an evaluation method for galloping in gusty wind. However, there has been little interest in this topic and little analytical work has been carried out.

This paper discusses differences between galloping in smooth wind and galloping in gusty wind through a numerical simulation focusing on their behavior rather than their mechanisms.

[†] Professor

[‡] Head

2. Background

2.1. Galloping mechanism

In power system, Lilien (1997) wrote: “we call ‘galloping’ any large amplitude, low frequency vibration, and these instabilities include both aerodynamic and aeroelastic aspects, which is not the case in civil engineering world (where they speak about torsional flutter, binary flutter, etc.).” As for galloping mechanisms, Lilien (1997) and Tunstall (1997) recently have given short reviews respectively and in the reference (Tunstall 1997) three categories of instabilities are identified :

1. A vertical instability requiring the C_L (the lift coefficient); and α (an angle of attack) characteristics of the iced profile to have a negative slope of sufficient magnitude (Den Hartog instability). This may be coupled to torsional motion via the aerodynamic moment and/or the ice eccentricity.
2. A two degree-of-freedom flutter involving vertical and torsional motion.
3. A torsional instability coupled to vertical motion.

In relation to category 2, ‘horizontal galloping’ has been occasionally observed, in particular, in Japan (Yukino *et al.* 1995). Lilien (1997) commented on this instability, “It is three degree of freedom galloping driven by torsion but especially with large amplitude when horizontal swinging frequency is close to half of vertical frequency (this last being close to torsional frequency). In such case the galloping mode has a shape of number eight”. In relation to category 3, Tunstall (1997) commented, “While torsional instability of single conductors has been observed, its origin is not clear. However, if the effective torsional frequency is very close to the vertical frequency, the lift variation generated by the change in α would lead to high vertical amplitude”.

The torsional frequencies of single conductors are much larger than the vertical values for similar numbers of loops unless the torsional frequency is reduced for some reason, such as the negative gravitational stiffness associated with an ice accretion lying above the axis of the conductor, the moment of inertia of an accretion and its aerodynamic moment characteristics (Tunstall 1997). On the other hand, the torsional frequencies of bundled conductors are much closer to the vertical values.

To discuss the mechanism, it is important to note the icing density and shape in relation to the torsional effect derived from the accretion, because characteristics of ice accretion are strongly dependent on local environmental conditions.

2.2. Galloping suppression device

Based on the galloping mechanism described above, to suppress galloping on a single or bundled conductor, it is necessary to improve the aerodynamic characteristics of the iced line and/or to control the effects of torsional oscillation. There are three types of ‘Galloping Suppression Device’. The first applies the idea of the detuning pendulum with (Lilien *et al.* 1993) / without an energy absorption concept. In the second, eccentric weights are attached horizontally to sub-conductors of a bundled line to produce an increment in the moment of inertia of the line. The natural frequency of each pendulum is thus made much higher than the vertical frequency of the bundled line, and the bundling is achieved using a ‘loose spacer’ that doesn’t restrict the rotation of the sub-conductors. The third one uses only a ‘special loose spacer’, which restricts the rotations of some sub-conductors of a bundled line and leaves others free (Ozawa *et al.* 1993).

Although many galloping suppression devices have been developed, they have been obtained by

trial and error approaches using full-scale tests. Thus, analytical approaches are anticipated. However, the approaches suggested are hard to achieve with vibrations that produce ‘large deformation’. In addition, few studies have discussed galloping in gusty wind.

3. Numerical approach

3.1. Analytical model

As a first step, this paper deals with the effects of wind turbulence on galloping by applying a numerical simulation method.

The analytical model assumes a line of Mogami Test Line consisting of a 4-bundled conductor on which triangular artificial icing models are attached (Ohkuma *et al.* 1998). This model spans 360 m and is supported at a height of 42 m. Steel towers at both ends of the line are assumed to be rigid and the 4-bundled conductor is modeled as an equivalent single conductor (Yamaoka *et al.* 1994).

Fig. 1 shows an overview of Mogami Test Line and the equivalent single conductor model. Fig. 2 shows wind coefficients of the 4-bundled conductor and Den Hartog criterion. It should be noted that the moment coefficient shows a negative slope in ranges of $\beta_S = 5\sim 20$ deg., $45\sim 70$ deg. and $170\sim 180$ deg., and values of the Den Hartog criterion become negative at $\beta_S = 20\sim 30$ deg. and $160\sim 170$ deg.

The equations of motion of the conductor are based on the Lagrangian formulations by Simpson (1972) and Yamaguchi *et al.* (1979), and they are made discrete in accordance with a finite element method in which ‘large deformation’ is taken into consideration. Here, it should be noted that it is inappropriate to model a transmission line as a chord, because a transmission line normally has a sag ratio of several percent. That is, its in-plane primary natural vibration mode is similar to the secondary mode of a chord, and it has a false loop in-plane natural vibration mode (Yamaguchi *et al.* 1979).

The authors have used the three dimensional analytical method, taking into account the transmission line’s geometrical non-linear properties. According to Lagrange’s equation of motion, in which the initial state is assumed as the under-dead-load state in the cable model, the translational component is :

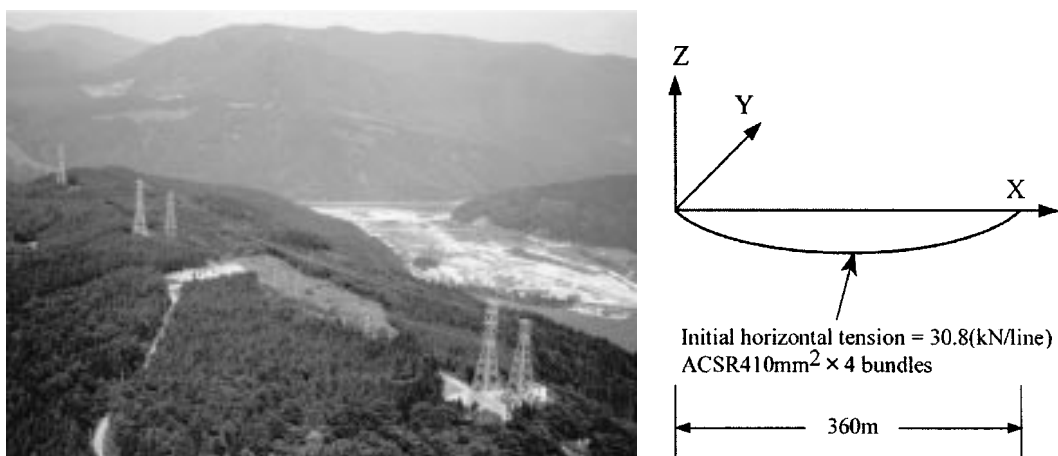


Fig. 1 Mogami Test Line and Equivalent single conductor model

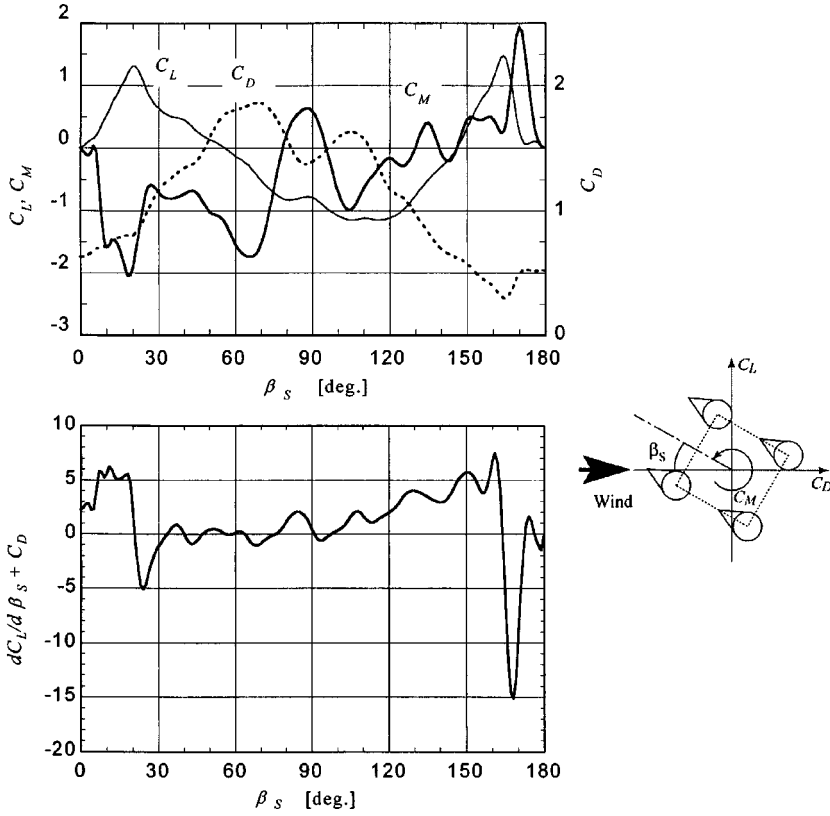


Fig. 2 Wind force coefficients of the 4-bundled conductor and Den Hartog criterion

$$-m \frac{\partial^2 X}{\partial t^2} - C_X \frac{\partial X}{\partial t} + \frac{\partial}{\partial s} \left\{ \frac{T}{1 + T/AE} \frac{\partial X}{\partial s} \right\} + F_X = 0 \tag{1}$$

$$-m \frac{\partial^2 Y}{\partial t^2} - C_Y \frac{\partial Y}{\partial t} + \frac{\partial}{\partial s} \left\{ \frac{T}{1 + T/AE} \frac{\partial Y}{\partial s} \right\} + F_Y = 0 \tag{2}$$

$$-m \frac{\partial^2 Z}{\partial t^2} - C_Z \frac{\partial Z}{\partial t} + \frac{\partial}{\partial s} \left\{ \frac{T}{1 + T/AE} \frac{\partial Z}{\partial s} \right\} + F_Z = 0 \tag{3}$$

and :

$$\left(\frac{\partial X}{\partial s} \right)^2 + \left(\frac{\partial Y}{\partial s} \right)^2 + \left(\frac{\partial Z}{\partial s} \right)^2 = \left(1 + \frac{T}{AE} \right)^2 \tag{4}$$

and the torsional component is :

$$-I \frac{\partial^2 \Theta}{\partial t^2} - C_\Theta \frac{\partial \Theta}{\partial t} + \frac{\partial}{\partial s} \left\{ \frac{GJ_P}{1 + T/AE} \frac{\partial \Theta}{\partial s} \right\} + M_\Theta = 0 \tag{5}$$

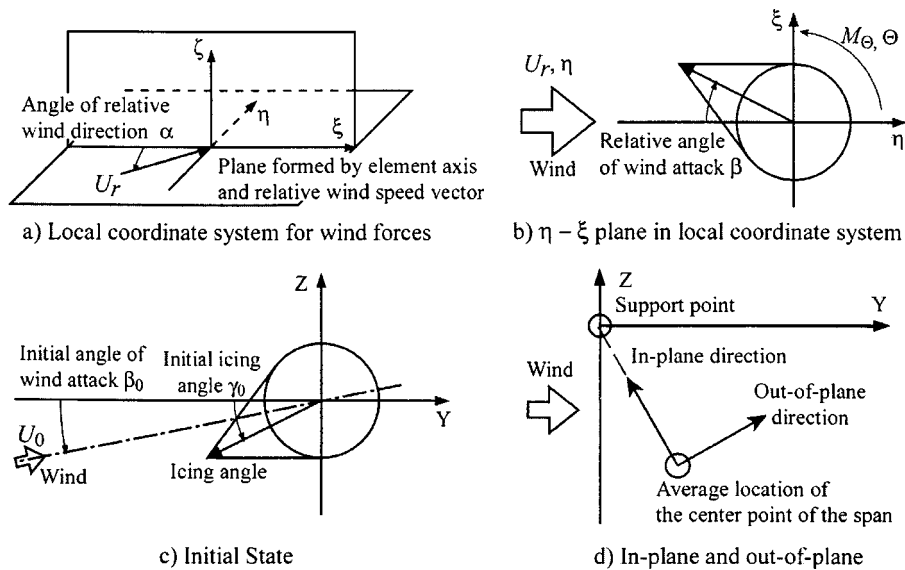


Fig. 3 Definition

where :

- T : time
- s : curvilinear coordinates parallel to the cable
- T : tension force
- AE : axial stiffness
- GJ_p : torsional stiffness
- X, Y, Z : Cartesian coordinate components in each direction
- Θ : torsional angle
- C_x, C_y, C_z, C_θ : structural damping coefficient in each direction of the unit length parallel to s
- m : mass per unit length parallel to s
- I : moment of inertia
- F_x, F_y, F_z : external force in each direction of the unit length parallel to s
- M_θ : torsional moment of the unit length parallel to s

The wind force is evaluated on the basis of the quasi-steady assumption. Fig. 3 shows the definitions of ‘local coordinate system for wind forces’, ‘initial state’ and ‘components of motions, in-plane and out-of-plane’, in which U_r stands for relative wind velocity and ξ is a coordinate which coincides with the axial direction of each conductor segment.

In the numerical calculation, values of damping constant (critical damping ratio) for translational and torsional motions of the conductor are assumed to be 4%, and the applied wind forces are evaluated on the basis of the quasi-steady assumption.

3.2. Galloping in smooth wind

Before discussing the effects of wind turbulence on galloping, the characteristic behaviors of galloping in smooth wind, i.e., uniform flow, are shown. Detailed parameter studies have verified that

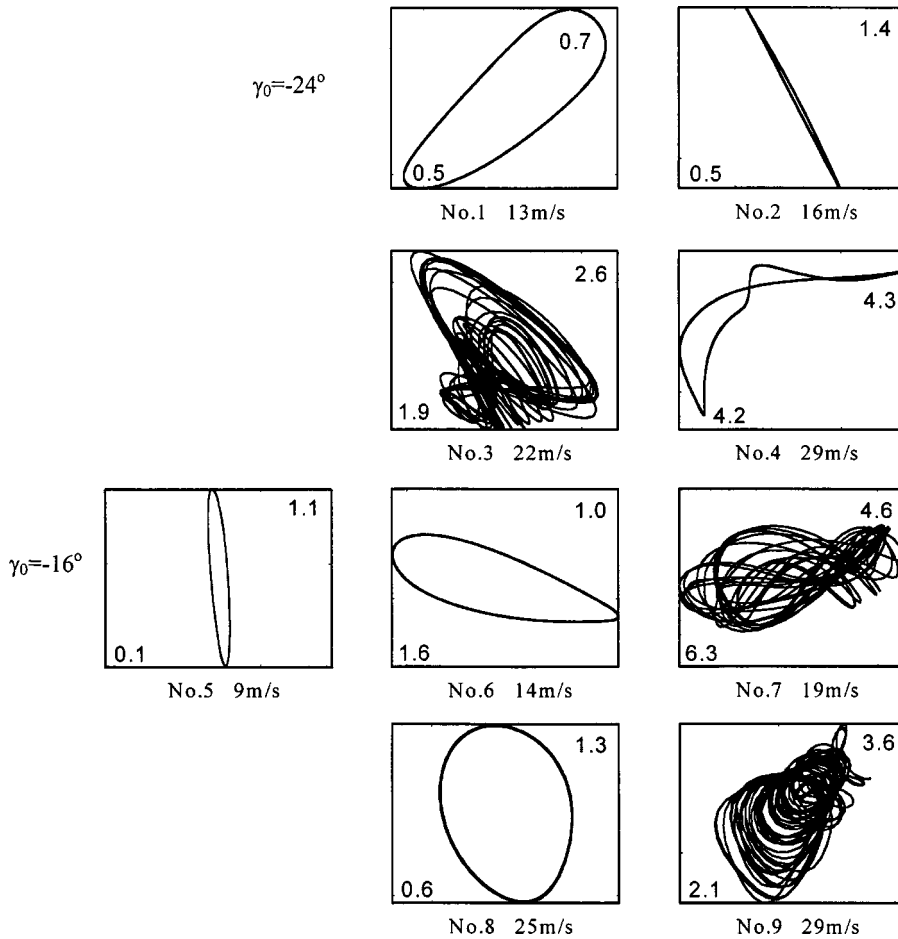


Fig. 4 Lissajous's figure of mid-span displacement ($\beta_0 = 0$)

vibration characteristics can in most cases be classified depending on values of both an initial relative angle of attack $\beta_0 - \gamma_0$, and a mean wind speed U (Ohkuma *et al.* 1998). Fig. 4 shows typical examples of Lissajous's figures of the conductor's displacement at mid-span, in which each numeral on the lower left (upper right) shows the maximum value in meters in a set of horizontal (vertical) components of total displacements of respective cycles for 10 min. Here, the lowest natural frequencies of the conductor under the condition of static wind loads corresponding to wind speeds of 10 to 30 m/s are 0.39 to 0.33 Hz for in-plane motion, 0.18 to 0.21 Hz for out-of-plane motion, and 0.25 to 0.28 Hz for torsional motion.

Interested points discovered are as follows (Ohkuma *et al.* 1998) :

- 1) The galloping in most cases occurs with in-plane and/or out-of-plane vibrations of the lowest natural frequencies with a combination of torsional vibration of the lowest natural frequency.
- 2) Depending on the initial relative angle of attack and the wind speed, Lissajous's figures of displacement can be classified into four types: a) vertically elliptic, b) horizontally elliptic, c) horizontally inclined figure-8, and d) others.

- 3) For example, Galloping of Nos. 2 and 5 are of the first type and they are based on the Den Hartog type.
- 4) Galloping of Nos. 1 and 6 are of the second type and they are swing-like vibrations with a torsional vibration, in which the characteristics of aerodynamic torsional moment play a key role.
- 5) Galloping of Nos. 3, 4 and 7 are of the third type and they are lateral-torsional coupled vibrations conducted by a torsional vibration. No. 7 shows a comparatively unsteady Lissajous's figure.
- 6) Galloping of Nos. 8 and 9 show different behaviors at positions on the conductor. In particular, a center of vibration in each cycle rolls for No. 9.

3.3. Galloping in turbulent wind

How does the behavior of galloping in smooth wind change with the addition of turbulence? Some characteristic behaviors of galloping in turbulent wind are introduced here. The turbulent wind considered is assumed to be a uniformly turbulent wind with a turbulence intensity $I_u = 15\%$ and $I_w = 7.5\%$, of which power spectra are defined as Karman type with a turbulence scale $L_u = 130$ m and coherences are of the exponential type with decay factor $C = 8$. The turbulence is produced using the AR method on the assumption of Gaussian process (Iwatani 1982).

Fig. 5 shows an example of Lissajous's figures of the conductor's displacement at mid-span. Here, Nos. 2T~9T correspond to Nos. 2~9, but in the turbulent wind.

The following effects of wind turbulence can be seen by comparing Fig. 5 with Fig. 4 :

- 1) For galloping with a steady Lissajous's figure such as No. 2, the predominant component isn't affected much while the center of displacement of each cycle drifts by long period fluctuations in wind velocity, particularly the along-wind component, as shown in No. 2T.
- 2) For galloping with a moderately steady Lissajous's figure such as Nos. 3 and 4, the amplitude of each cycle of predominant component varies randomly and the center of displacement of each cycle drifts as shown in Nos. 3T and 4T.
- 3) For galloping with an unsteady Lissajous's figure such as Nos. 7 and 9, in particular No. 9, which shows different behaviors at the conductor position, they almost change to random vibrations of the gust-induced type as shown in Nos. 7T and 9T.

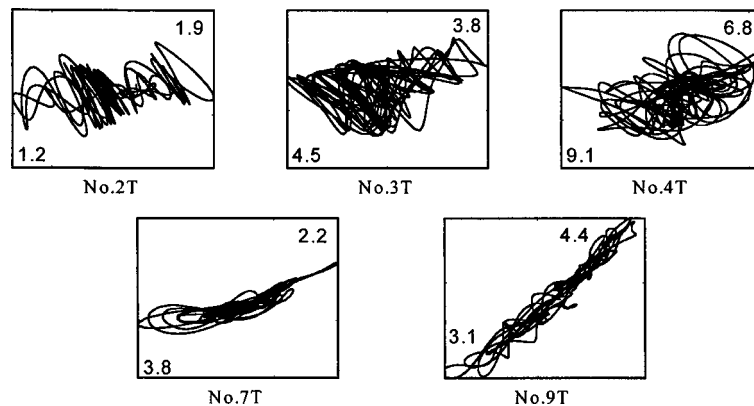


Fig. 5 Lissajous's figure of mid-span displacement

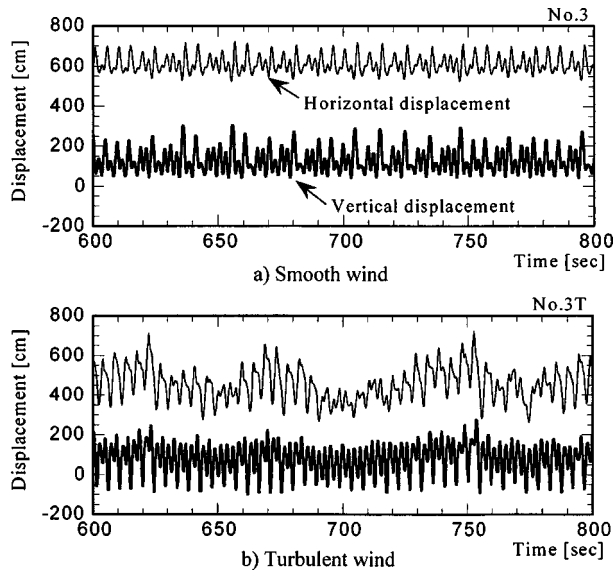


Fig. 6 Example of time series --- No.3 and No.3T

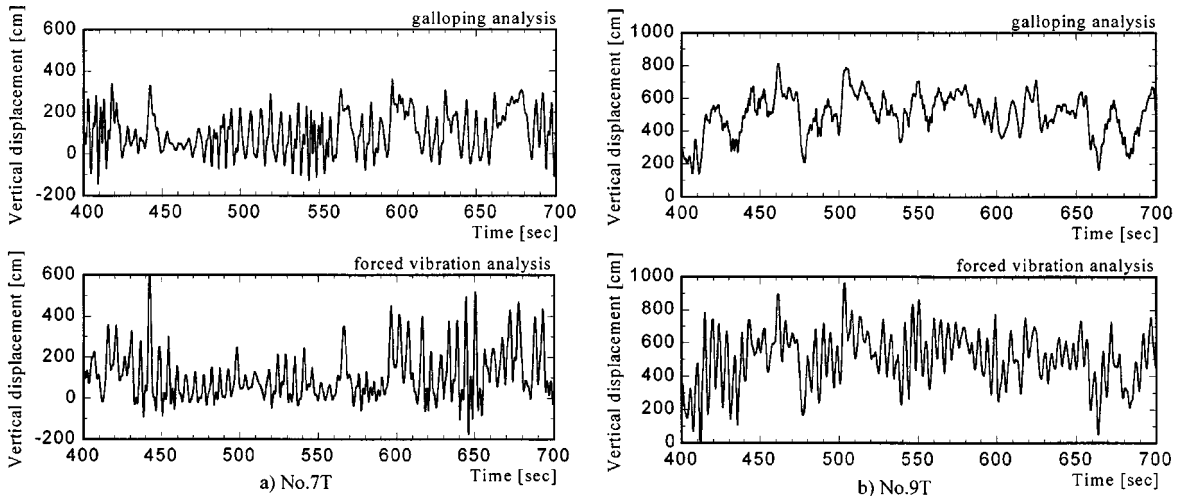


Fig. 7 Comparison of time series - galloping analysis and forced vibration analysis

Fig. 6 introduces part of a time series of No. 3 and No. 3T.

Fig. 7 compares the time series of vertical displacement at the center of the span in No. 7T and No. 9T with the response where the effects of the forces depending on the motion velocity are ignored (named forced vibration type here). The figure shows that galloping occurs temporarily in No. 7T. On the other hand, in No. 9T, the response based on the galloping analysis is shaped like the forced vibration response with its natural frequency component eliminated. No. 9T can be described as forced vibration generated by wind turbulence rather than as unstable oscillation such as galloping. Large differences between No. 7T and No. 9T are derived from that the aerodynamic positive damping force with strong intensity is induced in No. 9T.

3.4. Effects of wind turbulence

Referring to Fig. 5 and 6, galloping behaviors in gusty wind, $G(t)$, can be formulated as follows :

$$G(t) = D(t) + P(t) + r(t) \tag{6}$$

where, $D(t)$, $P(t)$, $r(t)$ are the drift component induced by the mean wind velocity and the long period fluctuation in wind turbulence, the predominant galloping component, and the other higher frequency random component, respectively.

To assess characteristic behaviors of respective components, a moving average operation was applied to behaviors of Nos. 2T, 3T, 4T, 7T and 9T with an averaging time of $1t_0 \sim 18t_0$ in which t_0 is 5sec. This value was chosen by taking into consideration that it is approximately equal to the value of the minimum predominant frequency, which is about 0.2 Hz. The analysis was made of the correlation between the alongwind velocity fluctuation and the conductor's displacement, particularly the vertical component, because preliminary results have shown that the effects of the across-wind component of wind velocity fluctuation are much smaller than those of the along-wind component.

Obtained major results are as follows :

- 1) The moving average displacements with an evaluation time of more than $12t_0$ of Nos. 2T, 3T, 4T, 7T and 9T correspond quite well to the results for smooth wind (see Fig. 8a, for example, in which the averaging time is $12t_0$, and the solid line shows the result for smooth wind), although all of them have a time lag of about 30 seconds behind the fluctuation of the moving average wind velocity.
- 2) The moving standard deviations of displacement with the evaluation time of more than $6t_0$ of Nos. 2T, 3T and 4T also correspond quite well to the results for smooth wind (see Fig. 8b with $6t_0$ of the averaging time), although all of them also have a timelag of about 30 seconds. However, good relationships weren't shown for Nos. 7T and 9T, because they are approximately random vibrations.

These averaged characteristics have been recognized in real galloping as shown in Fig. 9.

Lastly, the authors would like to emphasize that $G(t)$ and $r(t)$ components increase with the

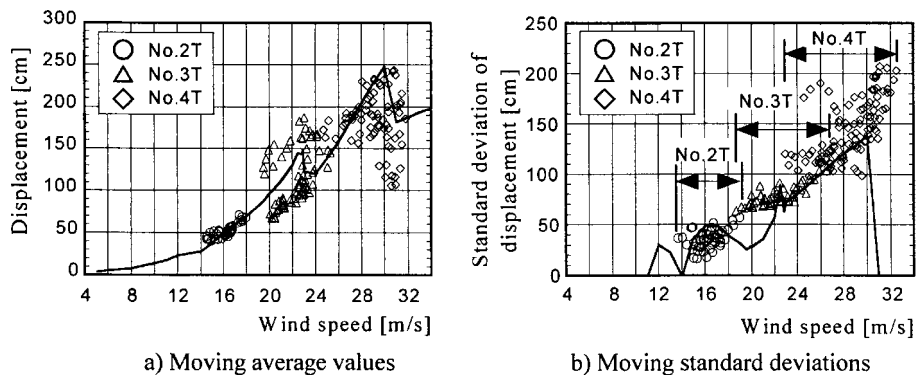


Fig. 8 Relationship, neglecting the time lag, between moving average values of wind velocity and moving average values/moving standard deviations of vertical displacement

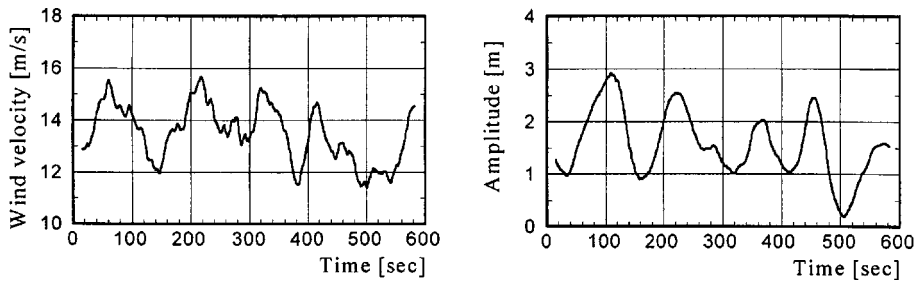


Fig. 9 Time history of averaged wind velocity and galloping amplitude with averaging time of ten times the galloping period

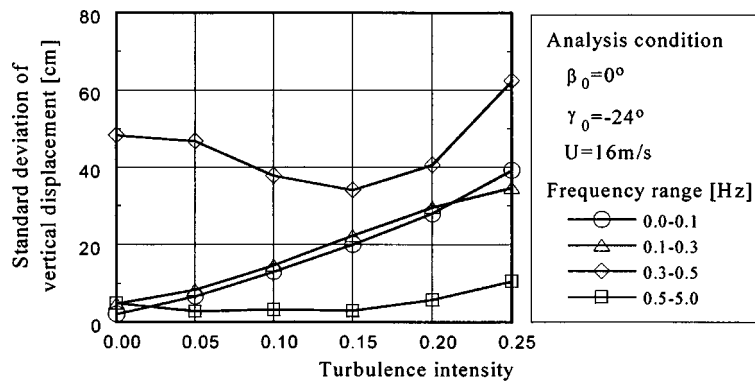


Fig. 10 Relationship between turbulence intensity and standard deviation of vertical displacement No. 2, No. 2T by frequency range

turbulence intensity, but the $P(t)$ component slightly changes within a turbulence intensity of about 20%, although it also increases for higher intensity turbulence. For example, see Fig. 10.

4. Conclusions

Gallop behaviors of overhead transmission lines seem to be strongly affected by wind turbulence. Accordingly, to effectively suppress galloping, it is necessary to develop more effective suppression devices not only for periodic vibrations but also for random vibrations (Lilien *et al.* 1993, Ozawa *et al.* 1999). It is also necessary to establish a more accurate evaluation method for galloping in gusty wind. Thus, the Institute of Electrical Engineers of Japan(IEEJ) started a technical research committee for estimation and suppression of galloping in 1998.

References

- EPRI (Electric Power Research Institute 1980), *Transmission Line Reference Book - Wind-Induced Conductor Motion*.
- IEEJ (1979), *Gallop of Transmission Line, Technical Report of IEEJ, Part II No.82*.
- Iwatani Y. (1982), "Simulation of multidimensional wind fluctuation having any arbitrary power spectra and cross spectra", *Journal of Wind Engineering, JAWE*, **11**, 5-19 (in Japanese).
- Lilien, J.L. (1997), "Gallop of overhead electrical lines - Mechanisms - Wind tunnel experiments - Field

- measurement”, *Proceedings of International Seminar on Cable Dynamics*, 37-48, Tokyo, October.
- Lilien, J.L. *et al.* (1993), “A new way to solve galloping on bundled lines - a concept, a prototype by two years field experience”, *CIGRE SC22 WG11 TFG*, Rep.93-04.
- Ohkuma, T. *et al.* (1998), “Numerical analysis of overhead transmission line galloping considering wind turbulence”, *The Trans. IEEJ of Japan - A Publication of Power and Energy Society*, **118-B**(12), 1386-1397 (in Japanese).
- Ozawa, A. *et al.* (1999), “Galloping suppressing effect of loose-spacer for 4-bundle conductor”, *Summaries of Annual Meeting of IEEJ*, 578-579 (in Japanese).
- Simpson, A. (1972), “Determination of the natural frequencies of multi-conductor overhead transmission lines”, *Journal of Sound and Vibration*, **20**(4), 417-449.
- Tunstall, M.J. (1997), “Wind-induced vibrations of overhead transmission lines - an overview”, *Proceedings of International Seminar on Cable Dynamics*, 13-26, Tokyo, October.
- Yamaguchi, H. *et al.* (1979), “Linear theory of free vibrations of an inclined cable in three dimensions”, *Journal of JSCE*, **286**(6), 29-36 (in Japanese)
- Yamaoka, M. *et al.* (1994), “Fundamental characteristics of overhead transmission line galloping by simulating calculation using equivalent single conductor method”, *Trans. IEE of Japan - A Publication of Power and Energy Society*, **144-B**(11), 1091-1098 (in Japanese).
- Yukino, T. *et al.* (1995), “Galloping phenomena of large bundle conductors observed on the full scale test line”, *Proceedings of International Symposium on Cable Dynamics*, 557-564 Liege, October.

(Communicated by Giovanni Solari)